Iranian Society of Acoustics and Vibration
The 14th ISAV2024 International Conference on Acoustics and Vibration
11-12 Dec 2024 Karaj - Iran
Kharazmi University

The effects of damping composite characteristics on maximizing modal damping ratio by topology optimization

Mahmoud Alfouneh

Department of Mechanical Engineering, Zabol University, Zabol, Iran
alfoone@uoz.ac.ir

Abstract

Reducing vibrations in the structure can be performed by damping composite materials. Maximizing the modal damping ratio (MDR) as a physical property of these materials can be a good tool to deal with it which can be performed by the topology optimization (TO). This paper studies many characteristics of composite damping materials of constraining layer damping structures (CLD) that affect maximizing MDR by TO. Mainly, it pays attention to characteristics such as Rayleigh damping coefficients, loss factor, elasticity modulus, volume fraction and the thickness of the damping layer. The TO method used here is the moving iso-surface threshold approach (MIST) which was applied successfully to some optimization problems. For each case, an illustrative example is presented and results are compared together to show the effectiveness of applying the method on how different factors can influence the MDR and vibration reduction. Specifically, it shows that adding more damping material does not guarantee that vibration reduction is achieved. In addition, an increase of the constraining layer damping leads to less effectiveness of the approach in vibration reduction of the multiplayer plate.

Keywords: MDR, topology optimization, moving iso-surface threshold, damping

1. Introduction

Different methods are employed to alleviate harmful vibrations on the structures. One of the methods is attaching a given amount of materials in the form of passive damping materials optimally by topology optimization (TO) in the advantage of no adding more weights[1]. MDR or modal loss factor are physical properties of the damping materials and can be considered as objective functions in TO. However, there are many characteristics of composite damping materials that influence the MDR and thereby the TO and distribution of damping materials.

TO has been applied frequently to address the vibration attenuation of the structures considering maximizing MDR or modal loss factor. In the study of Kim et al., [2] the optimal layouts derived by a heuristic topology optimization for loss factor maximization were compared to three other methods [3]. It was found that TO delivers about 61.14 percent larger modal loss factor. The eigenvector concept as a tool evaluating the damping loss factor was applied by Yamamoto et al., [4] and it was assumed that the eigenvectors with damping material were almost similar to the eigenvectors without damping material. The two-scale optimization approach is a technique that is used for maximizing MDR by topology optimization attained by the modal strain energy (MSE) method applied by Chen et al., [5] and Fang et al., [6]. MSE was also employed by Wang et. al., [7] and revised MSE by Xu et al., [8] in TO where the method utilized for an embedded and co-cured damping composite structure under the constraint of the total value of the experimental substance. It has resulted that the deleted elements in the structure correspond to the less sensitive elements in the sensitivity cloud.

In this paper, MIST topology optimization is employed to investigate the effects of different characteristics of composite damping materials such as Rayleigh damping coefficients, loss factor coefficient, thickness of layer damping and constraining layer, density of damping layer, and volume fraction on the maximizing MDR and then the optimal layout of the damping layer. Illustrative examples are presented to show the ability and validation of the method applied in this manuscript.

2. Statement

2.2 Damping layer optimization problem

As a consequence, we consider the problem of maximizing MDR for a chosen vibrational mode. The design goal is attained by optimizing the distribution of damping materials in the admissible design domain of the damping layer for the structure compromises of a host layer (elastic layer), an embedded damping layer, and a constraining damping layer. The structural damping is assumed to be Rayleigh $\bar{\mathbf{C}} = \alpha\bar{\mathbf{M}} + \beta\bar{\mathbf{K}}$ or non-proportional damping. $\bar{\mathbf{C}}$ is the damping matrix, $\bar{\mathbf{M}}$ is the mass matrix and $\bar{\mathbf{K}}$ is the stiffness matrix of the damping layer. α and β are Rayleigh damping coefficients.

The discretized optimization problem is formulated as follows:

$$\begin{aligned} &\text{find } \boldsymbol{\rho} = \{\rho_1, \rho_2, ..., \rho_e, ..., \rho_{nel}\} \quad (e = 1, ..., nel) \\ &\text{maximize: } \lambda_i \\ &\text{subject to} \\ &(\mathbf{K} - \omega^2\mathbf{M})\,\mathbf{X} = 0, \qquad \sum_{e=1}^{nel} \rho_e\, v_e \le V_0\, f\,, \qquad \varepsilon \le \rho_e \le 1, \qquad (e = 1, 2, 3, ..., nel) \end{aligned} \tag{1}$$

The symbol ρ_e expresses the volumetric density or weighting factor of the stiffer material in element *e* of the design domain of the damping layer which is meshed into *nel* elements and plays the role of the design variable in the problem. ρ is the vector of design variables. λ_i (*i*=1, 2, 3, …, *m*) is MDR of i^{th} mode with *m* being the ultimate number of modes. *f* is the maximum total fraction of stiffer material in the structure and it is less than one, V_0 is the volume of the admissible design domain and v_e is the volume of e^{th} element. ε is the lowest value of element density equal to 0.001, ω is the eigenvalue, **X** is the eigenvector, and **M** and **K** are the total mass and stiffness of the structure, respectively.

3. MDR definition

Damping in composite structure can be modeled in the classical damping model which considers Rayleigh damping coefficients and non-classical damping which considers loss factor η. MDR as a physical property of composite damping material is defined for different damping models as follows:

3.1 Classical damping model

For the classical damping model, the MDR is written as follows [9]:

$$\lambda_i = \int_{\Omega} (\bar{\alpha}^* \bar{T}_i(\boldsymbol{\rho}) + \bar{\beta}^* \bar{U}_i(\boldsymbol{\rho}) d\Omega \tag{2}$$

In which $\bar{\alpha}^* = \dfrac{\alpha}{\omega_i^3}$, $\bar{\beta}^* = \dfrac{\beta}{\omega_i}$ and $\bar{T}_i$, and $\bar{U}_i$ are respectively the modified Rayleigh damping coefficients and kinetic and strain energy density functions defined over the discretized design domain Ω and can be extracted from an FEM solver.

3.2 Non-classical damping model

For the non-classical damping model, the MDR can be given as [9]:

$$\lambda_i = \frac{\sum_{d=1}^{nd} \eta_d U_{vd}}{\sum_{s=1}^{ns} U_{bs} + \sum_{d=1}^{nd} U_{vd}} \tag{3}$$

where U_{vd} and U_{bs} are strain energies of the d^{th} and s^{th} layers, respectively if the structure consists of many damping and elastic layers. η_d is the loss factor of d^{th} damping layer and *b* and *v* stand for the base layer and damping layer.

4. Solution

To solve the topology optimization problem given in Eq.1, the MIST method is utilized. The MIST method was used previously for solving some optimization problems [10]. This method includes three key points: a) presenting an integral over design domain which is defined in terms of objective function and constraint b) representing an objective function by a physical response function Φ which is integrated over the design domain c) using a consecutive scheme applying the previous response of the structure for the solution of the next consecutive optimization problem. When a physical response function Φ is determined and constructed over the 2D design domain, a pre-calculated iso-surface threshold *t* derived through a bisection or sorting method of normalized and filtered design variables, cut the 3D physical response function surface to give and update element densities.

4.1 MIST formulation

As a vital part of the MIST method, Φ is defined as the integrand in Eq. 2 or U_{vd} in Eq. 3. When Φ is defined, the standard formulation of MIST for the optimization problem given in Eq.1 can be reformulated as follows:

$$\begin{aligned}
&\text{find } \boldsymbol{\rho} = \{\rho_1, \rho_2, ..., \rho_e\} \quad (e = 1, ..., nel) \\
&\text{maximize: } \lambda_i = \int_{\Omega} \Phi(\mathbf{x})\ h(t, \Phi)\ d\Omega \\
&\text{subject to} \\
&\quad (\mathbf{K} - \omega^2 \mathbf{M})\,\mathbf{X} = 0 \\
&\quad \int_{\Omega} h(t, \Phi)\ d\Omega \le f\, V_0, \qquad h(t, \Phi) = \begin{cases} 1 & \Phi \ge t \\ 0 & \Phi < t \end{cases}, \qquad \varepsilon \le \rho_e \le 1, \qquad (e = 1, 2, 3, ..., nel)
\end{aligned} \tag{4}$$

h is a homogenization function.

4.2 Algorithm

The whole numerical implementation procedure of the MIST iterative optimization scheme specialized for this problem consists of the following steps.

Step 1: Define the MIST parameters such as V_f, penalty factor, initial element densities, filter radius r_{min} and etc. More detail of the MIST can be found in the literature [11].

Step 2: Carry out modal analysis by ANSYS FEM platform to solve the first term of equilibrium Eq. 1 in conjunction with current or updated element densities and extract outputs for the next step.

Step 4: Calculate the objective function and find nodal values using an interpolation scheme or extrapolation over moving element patches applying a quadratic Lagrange interpolation [11];

Step 5: Normalize and filter the objective function values and calculate the iso-surface threshold.

Step 6: Construct the 3D physical response function and cut the 3D physical response function surface by the relevant iso-surface threshold *t* to derive the element densities or weighting factors.

Step 7: Update the element densities by proper move limit and element densities.
Step 8: Check the convergence where the difference between values of two sequential iterative steps becomes less than a prescribed low value else starts again from Step 2.

5. Examples and discussion

To illustrate the applicability and efficiency of the method a clamped three-layer plate shown in Fig. 1, is considered. The elastic layer has Young's module E=70MPa, material density ρ_0=2700kg/m^3, and Poisson's ratio ν=0.3. Material properties for the damping layer are: E=20MP, ρ_0=1140kg/m^3, ν=0.4, relevant α and β and η= in the case of non-classical damping in following examples. The constraining damping layer has material properties similar to the elastic layer. Each layer of the multilayer plate is discretized with 60×30 SOLSH190 ANSYS elements. For all the examples volume fraction is set equal to 0.5 otherwise it is mentioned in the right place. The filter radius r_{min}=0.0125 m and the penalty factor is 3. The move limit scheme is the dynamic move limit with an upper value of 0.2 and lower value of 0.0625 and it can become half when oscillation in variables occurs.

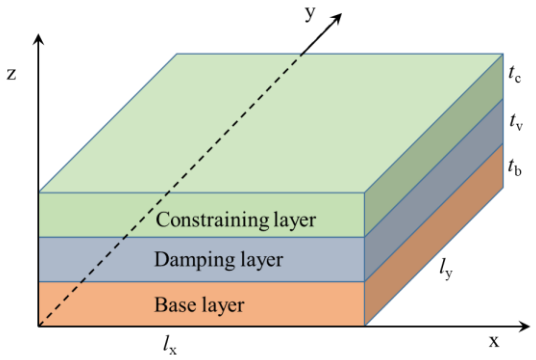

Fig. 1: A multilayer plate consists of a base layer, a damping layer, and a constraining layer.

5.1 Example 1: Rayleigh damping coefficients

In order to explore the impacts of α and β Rayleigh damping coefficients on the MDR, different values of α and β are applied and results are compared together in Fig. 2a for α damping and Fig. 2b for β damping on 5th mode. As can be seen, results for α damping are lower than β damping, and differences between the obtained MDR for different β damping are considerable though results for α=0 and β=0 are in the lowest positions. Clearly, the alpha damping coefficient variance of the damping layer in this range does not significantly alter the MDR.

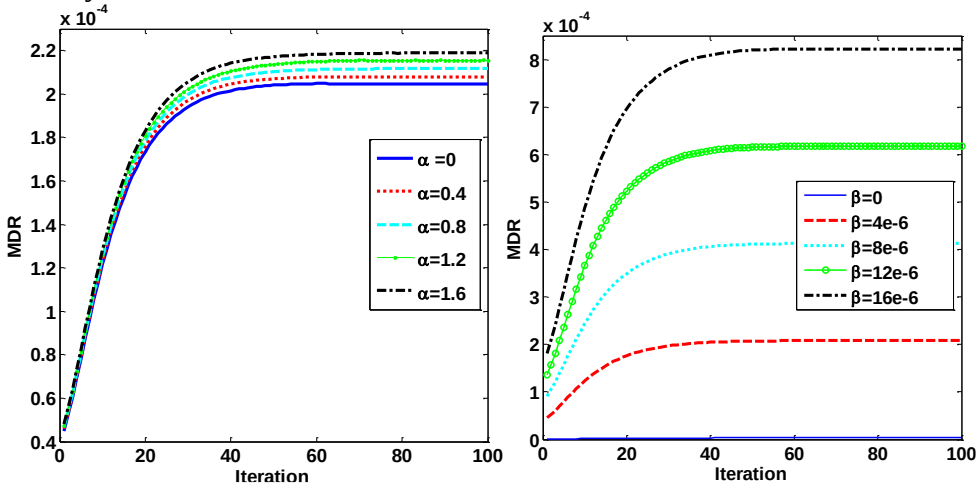

(a) (b)

Fig. 2: The influences of α and β on MDR results, a) results for α damping, b) results for β damping

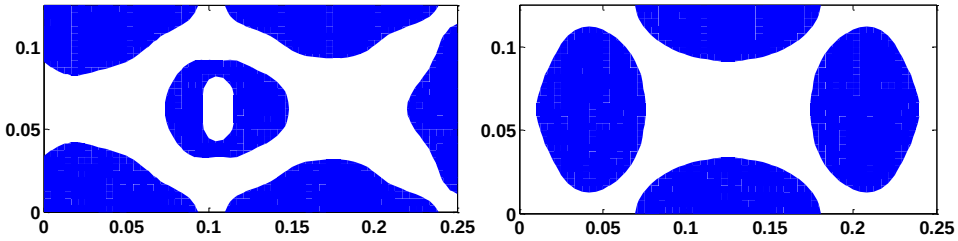

(a) (b)

Fig. 3: Optimal layouts of different α and β values, a)α and β optimal shapes, b) β=0.

Fig. 3a depicts the layout for different values of α and β which is the same for all of them except for the layout for β=0 which is seen in Fig 3b. It is observed that while more materials are seen connected to the edges in Fig. 3a, more materials are seen inside of design domain in Fig. 3b.

5.2 Example 2: Loss factor damping coefficient

Iteration histories of MDR for different loss factors of the multilayer plate given in the previous example to compare the effect of changing loss factor on the material distribution and MDR are denoted in Fig. 4a (α=β=0). It is evident from these figures that MDR maximization is strongly affected by the amount of loss factor. It is concluded that the maximum of MDR maximization is not achieved by high values of loss factor nor lower values but for η=2e-5. Though η=2e-6 as the lowest value of the study gives the lowest value of MDR maximization, η=2e-4 also acts the same. For each case of η optimal layout is derived and it is concluded that they are the same as the layout for the previous example for α studying.

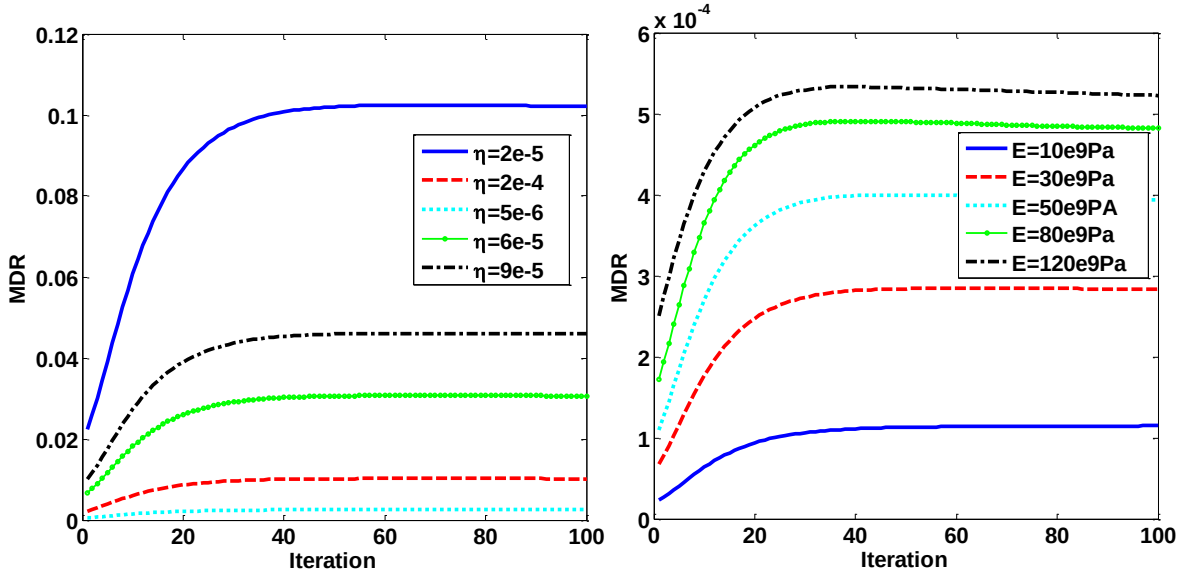

(a) (b)

Fig. 4: a)The effects of different loss factors on MDR, b)MDR variation during optimization process for the optimization of changing elasticity modulus.

5.3 Example 3: Elasticity modulus of damping layer

The objective of this example is to illustrate the change in elasticity modulus of the damping layer and its effect on the MDR maximization and layouts. Here, five elasticity moduli i.e., 10e9Pa, 30e9Pa, 50e9Pa, 80e9Pa, and, 120e9Pa are considered. The material properties and mode number are the same

as Example 1 except for α=0.4 and β=4e-7. Fig. 4b shows the curves of the MDR versus iteration number. The results reveal that by incrementing the elasticity modules of the damping layer, the amount of MDR has increased considerably. These results are anticipated since treatment in elasticity modulus impacts the system's kinetic and strain energy.

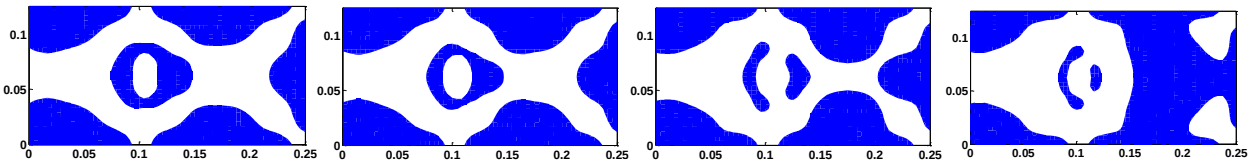

Fig .5: The optimal features of the damping layer for the optimization problem of changing the elasticity modulus of the damping layer. a) 10MPa and 30MPa, b)50MPa, c)80MPa, d)120MPa.

Figures 5a-5d depict the optimal features of the damping layer for elasticity modulus changing from 10MPa to 120MPa. It is observed that optimal layouts for lower elasticity modulus are approximately the same (10MPa to 30 MPa) while it changes significantly with elasticity modulus maximization.

5.4 Example 4: Damping layer thickness

To illustrate the application of the MDR method in the design of provided viscoelastic dampers for structures and compare the effect of the thickness of the damper layer on the overall damping of the structure, five different thicknesses are studied for the plate similar to the plate in Example 3 and results are shown in Fig. 6a. Although the total damping of the structure is maximized, it does not guarantee that the process of optimization is a maximization process where the MDR maximize from initial iteration to the last iteration number. It is observed that in lower and larger thicknesses, maximization of MDR happens while in mediocre thicknesses, MDR tends to be minimized.

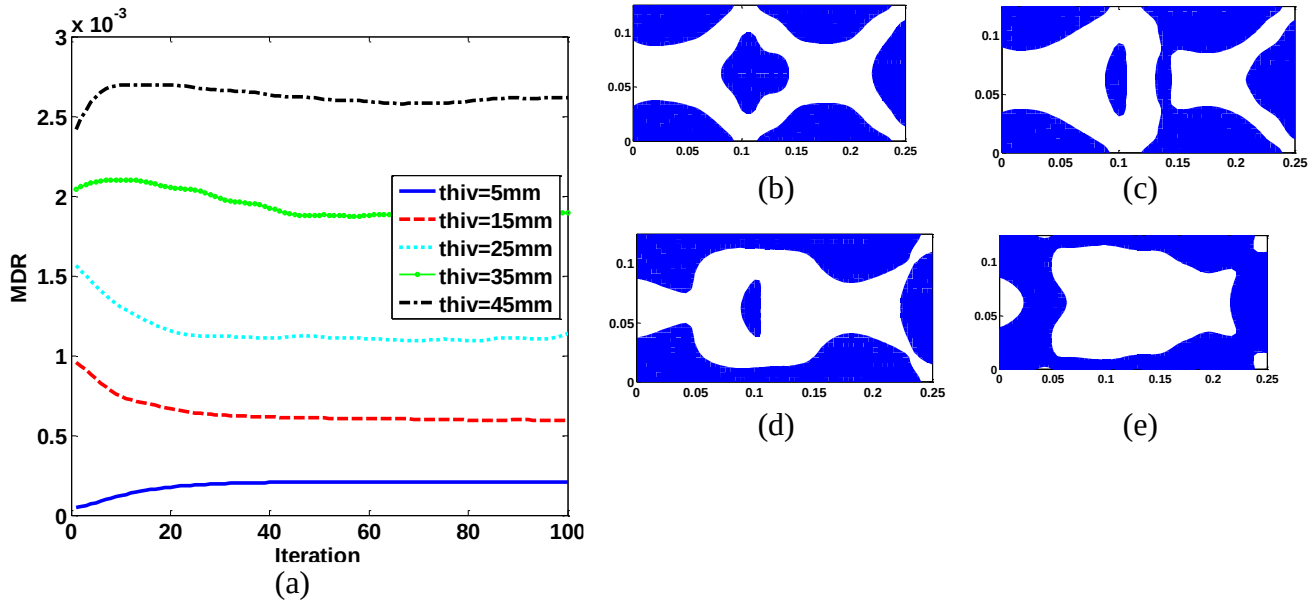

Fig. 6: a) MDR variations during optimization process for the optimization problem of different thicknesses of damping layer. Different optimal features of the damping layer with different thicknesses b)15mm, c)25mm, d)35mm, and e)45mm.

Optimal layouts with different features of coverage were obtained using the considered approach examined to determine the influence of the thickness of the damping layer on optimal layout and material coverage. As shown in Fig. 6b-6e for the case of thickness equal to 5mm, the layout obtained that gives the largest percent of maximization, the layout is analogous to Fig. 5a. As the amount of thickness is enlarged, part of the materials in the middle tend to vanish and materials are covering near the borders of the shape. On the other hand, the connection between parts of damping materials inside the design domain happens with the increase in thickness.

5.5 Example 5: Volume fraction

The example is used to look into the convergence of the approach and its capability to reproduce the solution of the maximum MDR, exploring the effect of volume fraction on convergence and optimal layouts. The same structure with similar material properties to Example 3 but different volume fractions i.e., V_f=0.1, 0.3, 0.6, and 0.8 is used. The optimization process is conducted and results are plotted in Fig. 7a. As can be demonstrated, results for V_f=0.1 and 0.8 are close to each other with some fluctuations assigned to the V_f=0.1. Further, there is a huge gap between results for V_f=0.3 and 0.1 in which results for V_f=0.1 are three times larger than results related to V_f=0.3.

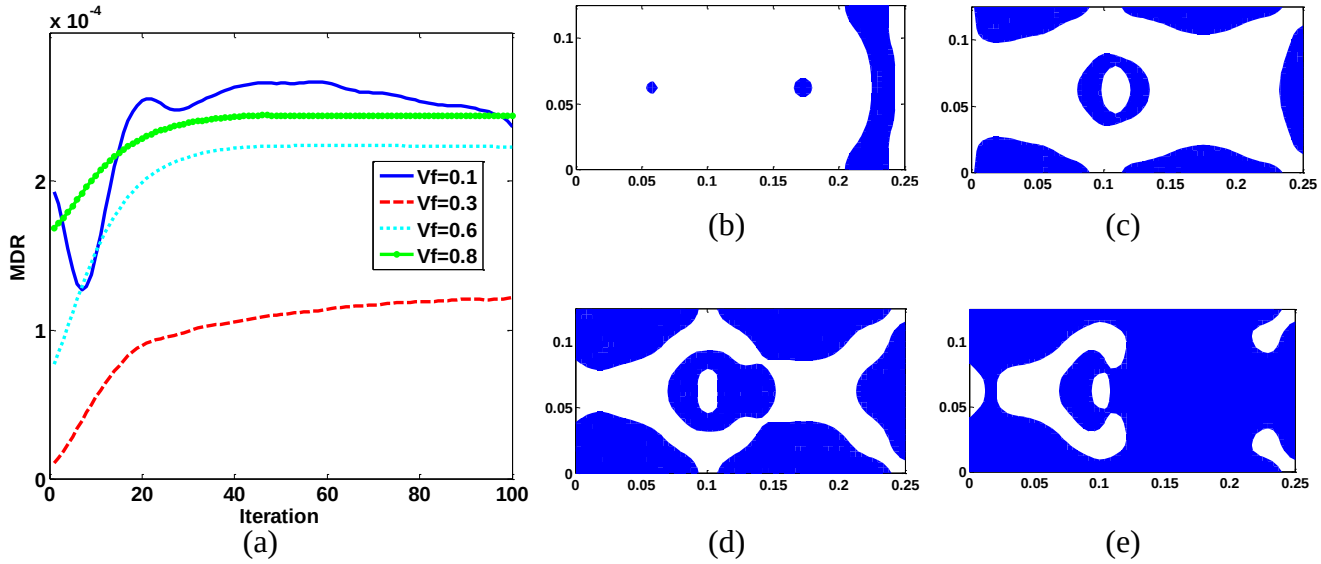

Fig.7: a) Comparison of MDR for different volume fractions. Comparison of optimal layouts for different volume fractions, b)V_f=0.1, c)V_f=0.3, d)V_f=0.6 and e)V_f=0.8..

As in the optimal layouts in Fig. 7b-7d, some diversities in figures are seen and materials tend to be covered at the right side by maximizing in volume fraction. Taking the figure for V_f=0,8, it resembles some features of the figure with V_f=0.6 in which materials that were distinct in Fig.7d are now connected to each other in Fig. 7e.

6. Conclusion

Five primary conclusions from this work are summarized as follows:

1) By comparing the impact of different α, β and η on the isotropic and laminated composite structure, it is concluded that the objective functions for α are quite close to each other; much less than ones for β values though objective functions for β values are maximized in conjunction with β increment. In the meantime, the objective functions for η decline with η increment. Further, the optimal shapes for α, β, and η are the same except for β=0.

2) Considering five different elasticity modulus, it is concluded that derived optimal features are different from each other, and obtained MDRs are maximized with the maximization of applied elasticity modulus.
3) For five cases of different thicknesses of damping layer, it is found that the process of optimization has not totally a maximization or minimization trend. While for lower values of thickness, MDR maximizes however it minimizes in larger thicknesses and most of the time derives the lesser objective functions in higher values of thickness. The optimal layouts are also different in which for the lower values of thickness, they are the same but they have different shapes in greater thicknesses.
4) The distribution of solid elements is influenced by the volume fraction of the design domain. In some cases, especially in lower values of volume fraction, large values of MDR are derived while in larger values of volume fraction, lower values of MDR are achieved. While in previous cases, the optimal shapes were somehow similar to each other, but in this case, they were totally different.
The strategy given here is a preliminary endeavor to solve the issue of topology optimization for laminated plates with design-dependent loads and is a promising scheme worthy of further investigation and application in this field.

7. References

1. Treviso, A., et al., *Damping in composite materials: Properties and models.* Composites Part B: Engineering, 2015. **78**: p. 144-152.
2. Kim, S.Y., C.K. Mechefske, and I.Y. Kim, *Optimal damping layout in a shell structure using topology optimization.* Journal of Sound and Vibration, 2013. **332**(12): p. 2873-2883.
3. Xia, L., et al., *Bi-directional evolutionary structural optimization on advanced structures and materials: a comprehensive review.* Archives of Computational Methods in Engineering, 2018. **25**(2): p. 437-478.
4. Yamamoto, T., et al., *Topology optimization of free-layer damping material on a thin panel for maximizing modal loss factors expressed by only real eigenvalues.* Journal of Sound and Vibration, 2015. **358**: p. 84-96.
5. Chen, W. and S. Liu, *Microstructural topology optimization of viscoelastic materials for maximum modal loss factor of macrostructures.* Structural and Multidisciplinary Optimization, 2016. **53**(1): p. 1-14.
6. Fang, Z., et al., *Concurrent Topology Optimization for Maximizing the Modal Loss Factor of Plates with Constrained Layer Damping Treatment.* Materials, 2022. **15**(10): p. 3512.
7. Wang, S., Q. Li, and S. Liang, *Topology optimization of embedded and co-cured damping composite structure.* Materials Research Express, 2020. **7**(10): p. 105102.
8. Xu, Y., Y. Liu, and B.S. Wang. *Revised modal strain energy method for finite element analysis of viscoelastic damping treated structures*. in *Smart Structures and Materials 2002: Damping and Isolation*. 2002. SPIE.
9. Alfouneh, M. and L. Tong, *Maximizing modal damping in layered structures via multi-objective topology optimization.* Engineering Structures, 2017. **132**: p. 637-647.
10. Luo, Q. and L. Tong, *Design and testing for shape control of piezoelectric structures using topology optimization.* Engineering Structures, 2015. **97**: p. 90-104.
11. Luo, Q. and L. Tong, *Structural topology optimization for maximum linear buckling loads by using a moving iso-surface threshold method.* Structural and Multidisciplinary Optimization, 2015. **52**(1): p. 71-90.